Ultrasound in Med. & Biol., Vol. 47, No. 3, pp. 679–692, 2021

0301-5629/$ - see front matter

https://doi.org/10.1016/j.ultrasmedbio.2020.11.022

● *Original Contribution*

VISUOMOTOR TRANSFORMATIONS ARE MODULATED BY FOCUSED ULTRASOUND OVER FRONTAL EYE FIELD

KALEB A. LOWE,[*,†,2] WOLF ZINKE,[*,†,2] M. ANTHONY PHIPPS,[‡,§] JOSH COSMAN,[*,†] MICALA MADDOX,[*,†] JEFFREY D. SCHALL,[*,†] and CHARLES F. CASKEY[†,§]

[*] Center for Integrative and Cognitive Neuroscience, Department of Psychology, Vanderbilt University, Nashville, Tennessee, USA; [†] Vanderbilt Vision Research Center, Department of Psychology, Vanderbilt University, Nashville, Tennessee, USA; [‡] Department of Radiology and Radiological Sciences, Vanderbilt University, Nashville, Tennessee, USA; and [§] Institute of Imaging Science, Department of Psychology, Vanderbilt University, Nashville, Tennessee, USA

(*Received* 5 *May* 2020; *revised* 16 *November* 2020; *in final from* 19 *November* 2020)

Abstract—Neuromodulation with focused ultrasound (FUS) is being widely explored as a non-invasive tool to stimulate focal brain regions because of its superior spatial resolution and coverage compared with other neuromodulation methods. The precise effects of FUS stimulation on specific regions of the brain are not yet fully understood. Here, we characterized the behavioral effects of FUS stimulation directly applied through a craniotomy over the macaque frontal eye field (FEF). In macaque monkeys making directed eye movements to perform visual search tasks with direct or arbitrary responses, focused ultrasound was applied through a craniotomy over the FEF. Saccade response times (RTs) and error rates were determined for trials without or with FUS stimulation with pulses at a peak negative pressure of either 250 or 425 kPa. Both RTs and error rates were affected by FUS. Responses toward a target located contralateral to the FUS stimulation were approximately 3 ms slower in the presence of FUS in both monkeys studied, while only one exhibited a slowing of responses for ipsilateral targets. Error rates were lower in one monkey in this study. In another search task requiring making eye movements toward a target (pro-saccades) or in the opposite direction (anti-saccades), the RT for pro-saccades increased in the presence of FUS stimulation. Our results indicate the effectiveness of FUS to modulate saccadic responses when stimulating FEF in awake, behaving non-human primates. (E-mail: charles.f.caskey@vanderbilt.edu)

Key Words: **Ultrasound, Neuromodulation, Frontal eye field, Visual search, Modulation.**

INTRODUCTION

Brain stimulation can be accomplished in a variety of forms either to study mechanisms of neural function (Nahas et al. 2001; Pollak et al. 2014) or to treat clinical disorders (Mayberg et al. 2005; Berényi et al. 2012). Direct electrical microstimulation, infusion of pharmacologic agents and chemogenetic techniques are effective for local modulation of brain activity but require invasive intracranial access. Electromagnetic stimulation, whether transcranial magnetic stimulation (TMS) or transcranial direct current stimulation (tDCS), can be applied non-invasively but is spatially non-specific. Acoustic stimulation has gained popularity because focused ultrasound stimulation (FUS) is non-invasive and spatially specific (Blackmore et al. 2019). However, the precise effects of FUS on focal regions are still unknown.

The frontal eye field (FEF) is an area of the frontal lobe that is defined functionally by the ability to evoke eye movements *via* intracortical electrical microstimulation (for review, see Schall 2015). The FEF contributes to the production of eye movements and allocation of visual spatial attention through the activity of neurons with spatially restricted receptive fields (Schall 2015). One task used to assess these functions is visual search. FEF neurons exhibit increased firing rates when the item in a search array that is located within their receptive field is a target and not a distractor. Given its very well characterized functional responses, FEF is an ideal candidate region for exploring the effects of FUS.

In previous non-human primate (NHP) studies, FUS was applied over the FEF through intact skull during an eye movement task requiring gaze shifts toward a visual

Address correspondence to: Charles Caskey, Department of Radiology and Radiological Sciences, Institute of Imaging Science, Vanderbilt University Medical Center, AA 1105 MCN, 1161 21st Avenue S, Nashville, TN 37232, USA. E-mail: charles.f.caskey@vanderbilt.edu

[2] K.A.L. and W.Z. contributed equally to this work.

target (pro-saccade) or away from the target (anti-saccade) (Deffieux et al. 2013; Wattiez et al. 2017). FUS application over the FEF has also been used in NHP studies to elicit saccadic choice biases in a simple two-alternative choice task (Kubanek et al. 2020). Here, we expand the use of FUS by applying stimulation during well-characterized visual cognitive tasks directly through a craniotomy, avoiding the attenuation and scattering of ultrasound when passing through bone. Three macaque monkeys performed visual search tasks during acoustic stimulation. We found that FUS consistently modulated response times for responses directed by stimuli contralateral to the stimulation site, as well as some response times and error rates for responses directed by stimuli ipsilateral to the stimulation site.

METHODS

Monkeys

Data were collected from three adult male macaque monkeys (*Macaca radiata*) (Ga: 9 y, 8.05 kg; He: 8 y, 8.35 kg; Da: 12 y, 8.9 kg). All procedures were in accordance with the National Institutes of Health's *Guide for the Care and Use of Laboratory Animals* and approved by the Vanderbilt Institutional Animal Care and Use Committee.

Behavioral task

Two monkeys, Ga and He, performed a shape-singleton visual search task. Both monkeys performed 14 sessions of the task and averaged 842 and 775 correct trials per session, respectively. Eye position was continuously monitored using an infrared eye tracker (EyeLink 1000, SR Research, Ottawa, ON, Canada) and streamed to a data acquisition system (MNAP, Plexon Inc., Dallas, TX, USA, or TDT Sys3, Tucker-Davis Technologies Inc., Alachua, FL, USA). The details of this task have been described previously (Cosman et al. 2018). In short, monkeys were presented with an array of eight gray-scale stimuli where a singleton L or T target shape was among seven T or L distractor shapes in one of four orientations (Fig. 1A). After a variable foreperiod, during

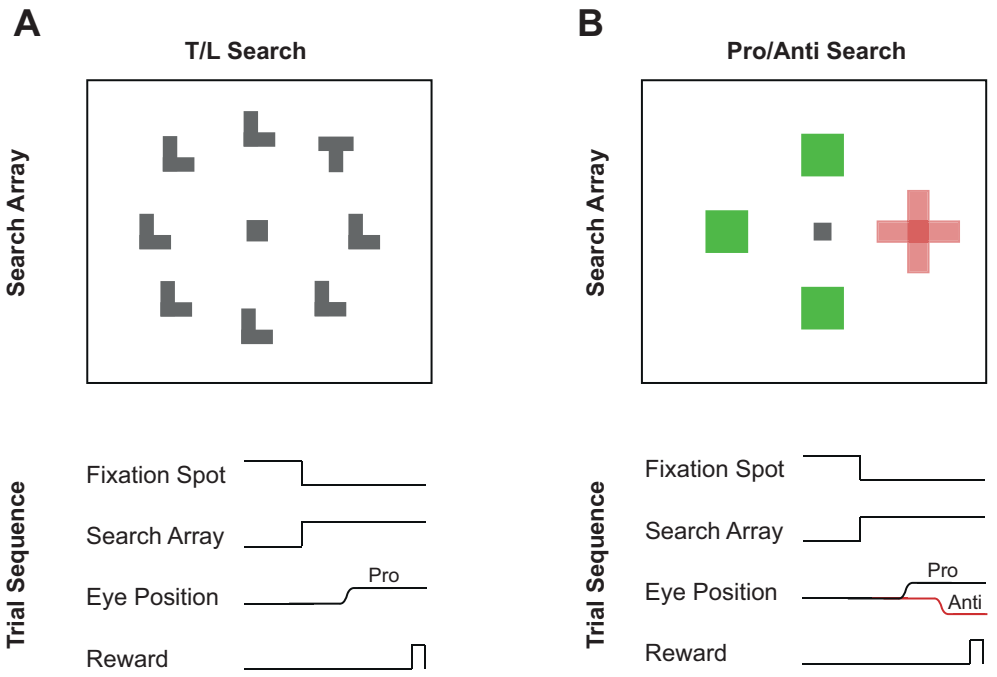

Fig. 1. Task diagrams. (A) Shape singleton search task. An example array (top) is shown with a singleton T among seven distractor L's. The trial sequence (below) indicates key trial events. The trial begins with a fixation spot on. After a delay, the fixation spot is extinguished and a search array appears. A saccade is made to the shape singleton, and fixation is maintained on it. If the target is successfully fixated for 200 ms, the reward is delivered. Saccades are always made toward the shape singleton, making them pro-saccades. (B) Pro-saccade/anti-saccade search task. The example array (top) is shown with a red singleton among three green distractors. The singleton is elongated and can be either vertical or horizontal. Additional trials in which the singleton was square and cued a no-go response were present but were not included in analysis. The two options are shown superimposed. The trial sequence (below) indicates key trial events. The trial begins with a fixation spot on. After a delay, the fixation spot is extinguished and a search array appears. If the color singleton is vertical, a pro-saccade is required (*black*). If the color singleton is horizontal, an anti-saccade is required, toward the stimulus across from it (*red*). If the correct stimulus is fixated for 1000 ms, the reward is delivered.

which the animal maintained its gaze on a fixation spot at the center of the screen, the stimulus array was presented and the monkey was required to make a saccade to the singleton target shape. Trials were aborted if the monkey broke fixation prematurely, made a saccade to an incorrect stimulus or broke fixation from the target prematurely after an initially correct saccade.

The third monkey, Da, performed a pro-saccade/anti-saccade search task (Sato and Schall 2003). Da performed 20 sessions of the task and averaged 1783 correct trials per session. In this task, four iso-eccentric stimuli were presented with even spacing (Fig. 1B). After a variable foreperiod, the array of stimuli was presented. All four stimuli had an area of 1 square degree of visual angle, presented at either 5° or 8°. One of the stimuli was a color singleton; either one red stimulus was presented among three green stimuli, or one green stimulus was presented among three red stimuli. The color singleton was either a square (aspect ratio = 1.0), a vertical rectangle (aspect ratio = 4.0) or a horizontal rectangle (aspect ratio = 0.25). The shape of this color singleton cued the task rule: if it was square then the monkey was required to maintain fixation on a central fixation stimulus for ~1.0 s (No-Go trial); if it was a vertical rectangle the monkey was required to perform a pro-saccade and fixate that color singleton (Pro trial); and if the rectangle was horizontal the monkey was required to perform an anti-saccade and fixate the stimulus located 180° away from the color singleton (Anti trial). Both pro-saccades and anti-saccades required the initial saccade to be performed within 2500 ms of array onset. If fixation was maintained at the correct location for 1000 ms, fluid reward was delivered. Otherwise, the trial was aborted and a 2000-ms time-out was added to the 1500-ms intertrial period.

Ultrasound stimulation

Recording chambers (Crist Instruments, Hagerstown, MD, USA) were placed over the FEF in all three monkeys (Ga and He had chamber implanted over the right hemisphere, while Da had the chamber over the left hemisphere). The sulcal pattern for each monkey is illustrated in Figure 2. Note that in monkeys Ga and Da, the chamber was centered on the rostral bank of the arcuate sulcus, the anatomic location of the FEF (Huerta et al. 1986, 1987; Stanton et al. 1988). However, in the third monkey, He, the center of the chamber lay slightly lateral to FEF.

A single-element piston transducer with a 2.54-cm-diameter, nominal focus of 5.08 cm, and 500-kHz center frequency was used for FUS sonications. A coupling cone was 3-D printed to attach the transducer to the

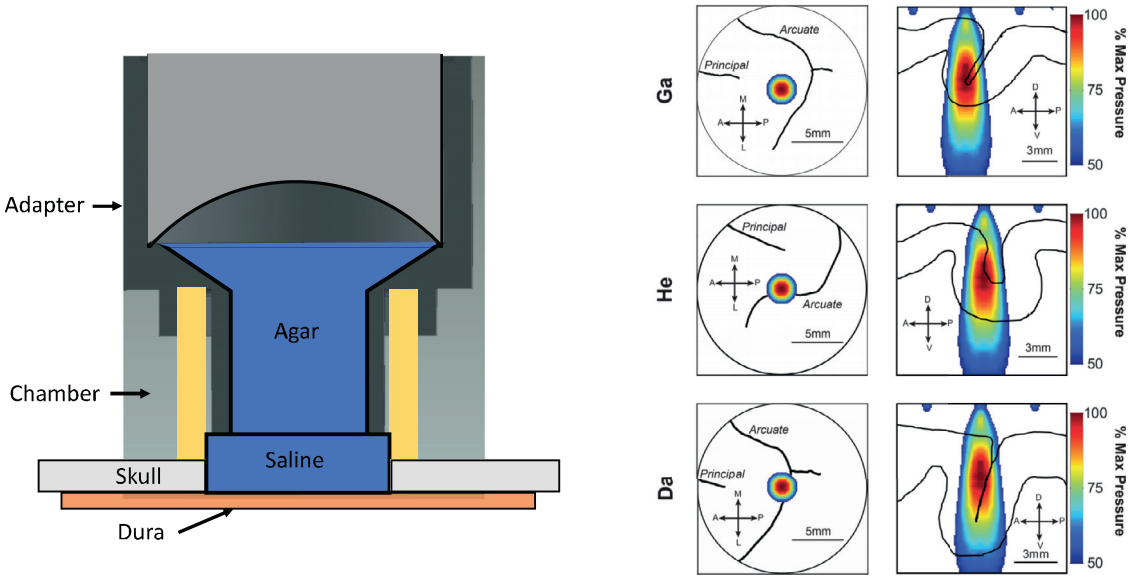

Fig. 2. Sulcal patterns of the three monkeys. Recording chambers were placed over the frontal eye field (FEF) of three monkeys. The interior circumference of the recording chamber is seen in the *circle*, and the sulcal pattern determined from anatomic magnetic resonance imaging is drawn in *black* (left). The principal and arcuate sulci are labeled as major landmarks. The FEF lies in the anterior bank of the arcuate sulcus. Sulcal patterns for Ga and He are reflected on the vertical axis such that all three monkeys are oriented with anterior to the left, posterior to the right, medial up and lateral down (inset). Beam intensity maps are superimposed. *Red* indicates maximum intensity, and *blue* indicates 50% of maximum intensity. Intensities below 50% of maximum are not shown. These sulcal patterns are reproduced in a sagittal section, showing depth (right). Anterior is to the left, posterior to the right, superficial up and deep down. Gray matter outlines are in *black*. Beam intensity maps are superimposed, with conventions as on the left.

recording chamber in a defined position (ProJet 3500 HDt, 3-D Systems, Rock Hill, SC, USA). The coupling cone extended into the recording chamber, stopping just above the brain. This cone was filled with a 1% weight per volume agar, and the recording chamber was filled with saline before fitting the FUS transducer in place to ensure acoustic coupling. Ultrasound was driven by a waveform generator connected to a radiofrequency amplifier. A microcontroller running a custom program was used to control the sonication pattern. A 300-ms block was pulsed at a maximum pulse repetition frequency of 0.33 Hz. This block consisted of 125 cycles pulsed at 2 kHz, yielding a 50% duty cycle within the block. The FUS pressure was calibrated by coupling the cone to a water tank with an acoustic window. A needle hydrophone (HNC-0400, Onda, Sunnyvale, CA, USA) was placed in the water tank at the opening of the coupling cone (where the brain surface would be during the experiment), and the pressure was recorded for a range of input voltages on the waveform generator. A calibration curve was determined from these data to identify voltages to achieve a peak negative pressure either at a low intensity (250 kPa) or high intensity (425 kPa). This experimental setup was also used to acquire a 2-D beam map coming out of the coupling cone, revealing the axial and lateral intensity profile of the beam. The beam map was acquired with 0.4-mm steps and was interpolated. Heat maps of beam intensity from 50% to 100% were then overlaid on anatomic brain images of the individual monkeys to estimate the beam location within the brain.

In monkeys Ga and He, ultrasonic stimulation was delivered in blocks of 10 min; 10-min blocks of trials had FUS delivered in a 300-ms window centered on the time of array onset, and these blocks alternated with blocks during which no FUS was delivered. One-half of the session used an FUS stimulation with low intensity (250 kPa), and the other half, with high intensity (425 kPa). The order of FUS intensities was alternated between sessions. On average, sessions were 138 min long, allowing for 3.5 alternations between FUS and no-FUS blocks per intensity per session. In monkey Da, ultrasonic stimulation was randomly delivered on 50% of trials and began at the time of array onset.

Data analysis

Data analysis was performed using custom MATLAB scripts (The MathWorks Inc., Natick, MA, USA). Response times were determined offline as the time at which the eye velocity exceeded two standard deviations of the eye velocity in the time before array onset. To assess whether FUS effects were spatially specific, RT differences were tested with an analysis of variance (ANOVA) with target location and stimulation intensity as factors. Target location was expressed either as the polar angle from the fixation point or as ipsilateral or contralateral to the FUS site. To assess whether FUS affected behavior in the T/L search task, the response times were assessed *via* paired t-test. Because ipsi- and contralateral stimulus presentations were presented in the same session, both with and without FUS, the mean differences in RT for FUS and no-FUS conditions were tested separately for each hemifield and each monkey. We found no differences between FUS intensities, so these sessions were combined for further analysis. In the T/L search task, ipsi- and contralateral labels of trial types are identical whether the label applies to the singleton location or the saccade direction. The logit transform was applied to error rates before *t*-tests or ANOVAs.

To assess whether FUS affected behavior in the pro-saccade/anti-saccade search task, the response times were assessed in a four-way ANOVA with factors of stimulation (present or absent), singleton location (ipsi- or contralateral to the hemisphere of FUS stimulation), saccade rule (pro- or anti-saccade) and FUS intensity (250 or 425 kPa). After the omnibus ANOVA, which suggested a significant effect of FUS on RT (see Results), and because FUS and non-FUS trials were present within the same session, the effect of FUS was assessed *via* paired *t*-test. The differences in mean RT and error rates were tested against zero separately for ipsi- and contralateral stimulus presentations in both pro- and anti-saccade trials. Importantly, in this task ipsi- and contralateral singleton locations cue ipsi- and contralateral saccades, respectively, on pro-saccade trials only. On anti-saccade trials, ipsilateral singleton locations cue contralateral saccades, and contralateral singleton locations cue ipsilateral saccades. Thus, labeling of trials as ipsi- or contralateral differs on anti-saccade trials depending on whether the label applies to the stimulus or saccade. As effects of FUS are most consistent for contralateral stimulus locations, but not specifically contralateral saccades (see Results), we label trials with respect to the singleton location, not saccade direction. This contrasts with other anti-saccade studies of FUS (Deffieux et al. 2013; Wattiez et al. 2017), but allows for a more parsimonious description of effects.

RESULTS

Ultrasound modulation of shape singleton search behavior

Two monkeys performed a shape singleton search task during focused ultrasound stimulation. We found that FUS affected response times in the shape singleton search task (Fig. 3A−C). For monkey Ga, the mean response time across all conditions was 127 ± 4.1 ms; thus, responses were produced before the end of stimulation on 92.6 ± 2.7% of trials. For monkey He, on the

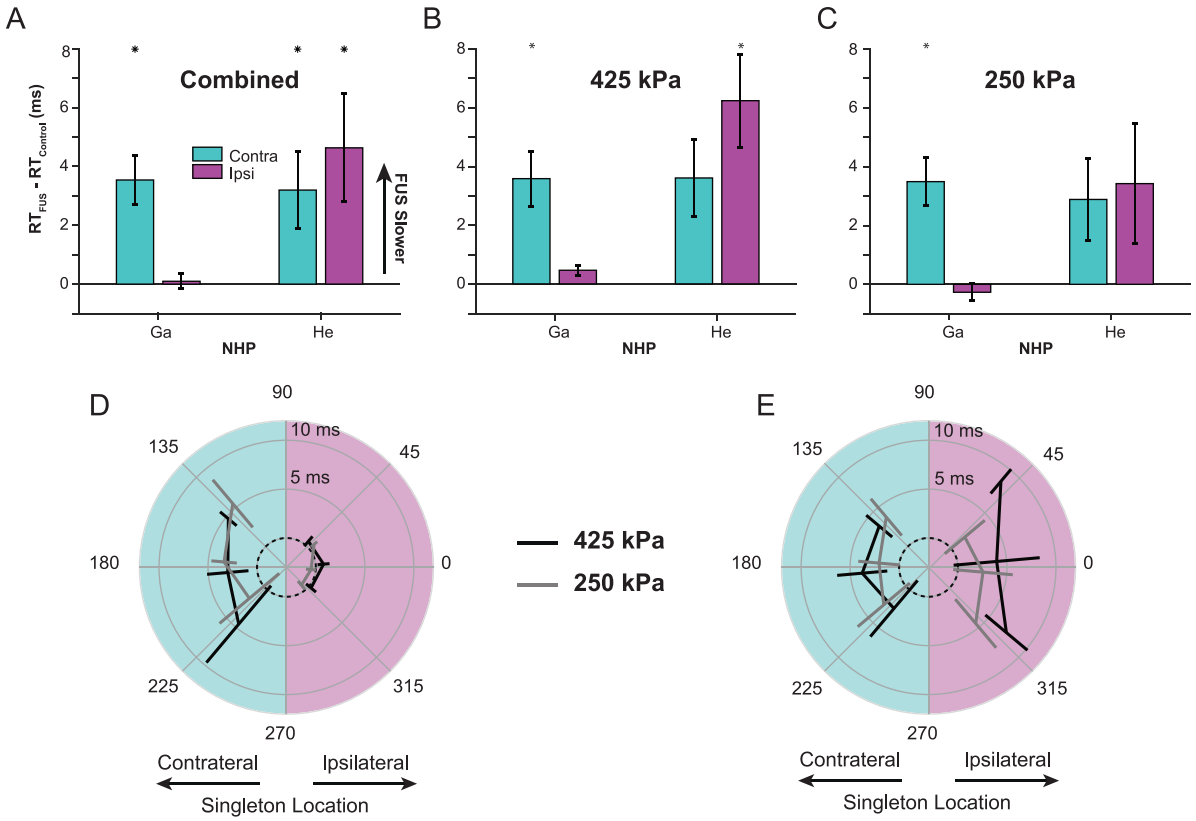

Fig. 3. Average performance for shape singleton search task. (A) The average differences ± standard error of the mean (SEM) for response times are shown for each monkey, labeled on the abscissa. Contralateral shape singletons are shown on the left of each pair, in *cyan*, and ipsilateral shape singletons are shown on the right of each pair, in *magenta.* Longer response times (RTs) in the focused ultrasound (FUS) condition relative to the no-FUS condition are plotted upward. Asterisks mark significant differences from zero ($p < 0.05$). (B) The average differences ± SEM for response times during the high-intensity (425 kPa) trials are shown for each monkey. Conventions as in (A). †Trend toward significance ($p < 0.1$). (C) The average differences ± SEM for response times during the low-intensity (250 kPa) trials are shown for each monkey. Conventions as in (B). (D) Average RT differences ± SEM for monkey Ga at each target location are shown. High-intensity sessions are shown in *black*, and low-intensity sessions in *gray*. A *dashed black line* at a 0-ms difference (no effect) is shown for reference. (E) Average RT differences ± SEM for monkey He at each target location are shown. Conventions as in (D).

other hand, the mean response time across all conditions was 167.9 ± 12.7 ms; thus, responses were produced before the end of stimulation on only 36.4 ± 11.3% of trials. At high FUS intensity, monkey Ga had slower response times for singleton locations contralateral to the FUS stimulation site (mean difference ± standard error of the mean [SEM]: 3.59 ± 0.94 ms; $t[6] = 2.71$, $p = 0.035$), but not for singleton locations ipsilateral to the FUS stimulation site (mean difference ± SEM: 0.46 ± 0.17 ms; $t[6] = 1.90$, $p = 0.106$). Monkey He had slower response times for singleton locations ipsilateral to the FUS stimulation site (mean difference ± SEM: 6.24 ± 1.58 ms; $t[6] = 2.58$, $p = 0.049$) but not for singleton locations contralateral to the stimulation site (mean difference ± SEM: 3.61 ± 1.30 ms; $t[6] = 1.81$, $p = 0.130$). At low FUS pressure (250 kPa), monkey Ga had slower response times for singleton locations contralateral to the FUS stimulation site (mean difference ± SEM: 3.49 ± 0.80 ms; $t[6] = 3.07$, $p = 0.022$) but not for singleton locations ipsilateral to the FUS stimulation site (mean difference ± SEM: −0.27 ± 0.29 ms; $t[6] = -0.66$, $p = 0.532$). Monkey He did not have different response times for either contralateral (mean difference ± SEM: 2.89 ± 1.40 ms; $t[6] = 1.56$, $p = 0.162$) or ipsilateral (mean difference ± SEM: 3.43 ± 2.05 ms; $t[6] = 1.26$, $p = 0.247$) singleton locations.

To assess whether these effects were statistically different by location or by intensity, we performed an ANOVA with factors of location and stimulation intensity. For monkey Ga, when location was expressed as polar angle of the target location, we found that neither location ($F[5,72] = 1.78$, $p = 0.127$) nor intensity ($F[1,72] = 0.194$, $p = 0.6611$) affected the magnitude of the RT effect. When location was expressed as the

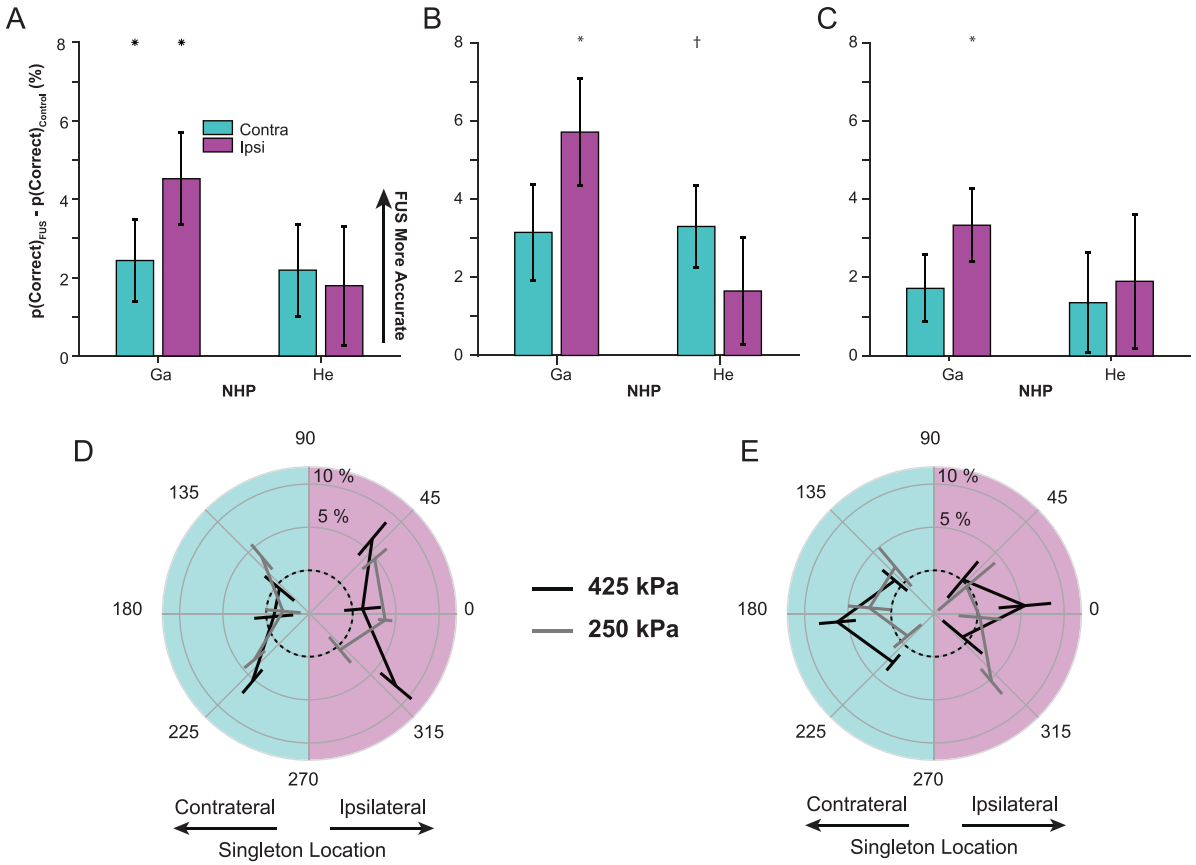

Fig. 4. Average error rates for shape singleton search task. The average differences ± standard error of the mean (SEM) for error rate are shown. Conventions as in Figure 3. Increased accuracy in the focused ultrasound (FUS) condition relative to the no-FUS condition is plotted upward.

hemifield relative to the stimulation site, we found that hemifield ($F[1,80] = 8.51$, $p = 0.005$) but not intensity ($F[1,80] = 0.21$, $p = 0.648$) affected the magnitude of the RT effect. For monkey He, when location was expressed as polar angle, we found that neither location ($F[5,72] = 0.38$, $p = 0.860$) nor intensity ($F[1,72] = 1.37$, $p = 0.247$) affected the magnitude of the RT effect. When location was expressed as hemifield, we found that neither hemifield ($F[1,80] = 1.05$, $p = 0.309$) nor intensity ($F[1,80] = 1.48$, $p = 0.228$) affected the magnitude of the RT effect, contrary to the result for monkey Ga.

Because we did not observe an effect of stimulation intensity, we repeated the analyses by combining across both FUS intensities. When intensities were combined, monkey Ga had slower response times for singleton locations contralateral to the FUS stimulation site (mean difference ± SEM: 3.54 ± 0.84 ms; $t[13] = 4.22$, $p = 0.001$) but no difference for ipsilateral singleton locations (mean difference ± SEM: 0.10 ± 0.25 ms; $t[13] = 0.39$, $p = 0.7039$). Monkey He had delayed response times for both contralateral singleton locations (mean difference ± SEM: 3.20 ± 1.31 ms; $t[13] = 2.44$, $p = 0.0296$) and ipsilateral singleton locations (mean difference ± SEM: 4.63 ± 1.84 ms; $t[13] = 2.52$, $p = 0.0255$).

Effects were also observed in error rates (Fig. 4A–C). At the high FUS intensity, monkey Ga had increased accuracy for singleton locations ipsilateral to the FUS stimulation site (mean difference ± SEM: 5.7 ± 1.4%; $t[6] = 3.07$, $p = 0.022$), but not contralateral (mean difference ± SEM: 3.2 ± 1.2%; $t[6] = 1.90$, $p = 0.107$). Monkey He had a trend toward increased accuracy for singleton locations contralateral to the FUS stimulation site (mean difference ± SEM: 3.3 ± 1.1%; $t[6] = 2.12$, $p = 0.088$) but not ipsilateral (mean difference ± SEM: 1.7 ± 1.4%; $t[6] = 0.42$, $p = 0.689$). At the low FUS intensity, monkey Ga had increased accuracy for singleton locations ipsilateral to the FUS stimulation site (mean difference ± SEM: 3.3 ± 0.93%; $t[6] = 2.77$, $p = 0.032$) but not contralateral (mean difference ± SEM: 1.72 ± 0.85%; $t[6] = 1.51$, $p = 0.181$). Monkey He did not have different accuracy for either contralateral (mean difference ± SEM: 1.36 ± 1.28%; $t[6] = 0.722$, $p = 0.494$) or ipsilateral (mean difference ± SEM: 1.90 ± 1.71%; $t[6] = 1.57$, $p = 0.160$) singleton locations.

To assess whether these effects were statistically different by location or by intensity, we performed an ANOVA with factors of location and stimulation intensity. For monkey Ga, when location was expressed as polar angle of the target location, we found that location affected the magnitude of the accuracy effect ($F[5,72]) = 3.15$, $p = 0.013$) but intensity did not ($F[(1,72] = 0.614$, $p = 0.436$). When location was expressed as the hemifield relative to the stimulation site, we found that hemifield ($F[1,80] = 4.58$, $p = 0.035$) but not intensity ($F[1,80] = 0.54$, $p = 0.467$) affected the magnitude of the accuracy effect. For monkey He, when location was expressed as polar angle, we found that neither location ($F[5,72] = 0.67$, $p = 0.647$) nor intensity ($F[1,72] = 0.33$, $p = 0.567$) affected the magnitude of the accuracy effect. When location was expressed as hemifield, we again found that neither hemifield ($F[1,80] = 0.10$, $p = 0.754$) nor intensity ($F[1,80] = 0.329$, $p = 0.568$) affected the magnitude of the accuracy effect.

Again, because we did not observe an effect of stimulation intensity, we repeated the analyses by combining across both FUS intensities. When intensities were combined, monkey Ga had increased accuracy for both contralateral singleton locations (mean ± SEM: 2.4 ± 1.0%; $t[13] = 2.46$, $p = 0.0285$) and ipsilateral singleton locations (mean ± SEM: 4.5 ± 1.2%; $t[13] = 4.11$, $p = 0.0012$). These effects were not different for targets on either hemifield (mean ± SEM: 2.1 ± 5.2%; $t[13] = 1.51$, $p = 0.1543$). Monkey He exhibited no difference in accuracy for either contralateral singleton locations (mean ± SEM: 2.2 ± 1.2%; $t[13] = 1.67$, $p = 0.1188$) or ipsilateral singleton locations (mean ± SEM: 1.8 ± 1.5%; $t[13] = 1.59$, $p = 0.1351$).

To further probe the nature of the effect of FUS on response times, we divided the RT distributions from each session and each condition into quantiles. This allowed a comparison of the effect of FUS at short, intermediate and long RTs. We calculated a correlation between the difference in FUS and no-FUS trials and RT quantile (Fig. 5). No differences were found for any monkey or singleton locations (Ga, contra: $r[124] = -0.01$, $p = 0.9119$; Ga, ipsi: $r[124] = 0.04$, $p = 0.6306$; He, contra: $r[124] = -0.06$, $p = 0.5341$; He, ipsi: $r[124] = -0.07$, $p = 0.4179$). Thus, the effects of FUS stimulation were consistent across RT distributions.

Ultrasound modulation of pro-saccade/anti-saccade search behavior

We have found that FUS can affect response times during visual search when applied to the FEF. However, these effects were small, less than 10 ms. Previous studies have indicated that FUS stimulation of the FEF can affect response times in anti-saccade tasks on the order of tens of milliseconds (Deffieux et al. 2013; Wattiez et al. 2017). To increase the cognitive load in the search task to perhaps magnify the effects, as well as to replicate the findings of FUS in anti-saccades, the third monkey performed the pro-saccade/anti-saccade search task. In this task, FUS stimulation occurred in 50% of trials. Because anti-saccade trials dissociate singleton location and saccade direction, we label trial types with respect to the singleton location. Thus, our contralateral anti-saccade trials are those in which a contralateral singleton cues an ipsilateral saccade. The mean response time across all conditions was 580.2 ± 44.8 ms; thus, the stimulation ended after the response on 54.3 ± 4.3% of trials. We again found that RTs were affected by stimulus−response mapping rule ($F[1,144] = 99.37$, $p < 0.001$), singleton location ($F[1,144] = 361.18$, $p < 0.001$) and FUS ($F[1,144] = 8.29$, $p = 0.0046$). Given the overall effect of FUS on RT, we performed four paired *t*-tests for each FUS pressure (Fig. 6). We found that at the high pressure (425 kPa), RTs were significantly longer in anti-saccades directed by a singleton contralateral to the FUS stimulation site (mean difference ± SEM: 31.5 ± 11.3 ms; $t(9) = 2.80$, $p = 0.021$) but not ipsilateral (mean difference ± SEM: 1.5 ± 4.5 ms; $t[9] = -0.33$, $p = 0.748$). RTs trended toward being longer in pro-saccades directed by an ipsilateral singleton location (mean difference ± SEM: 11.0 ± 5.6 ms; $t[9] = 1.96$, $p = 0.081$) but not contralateral (mean difference ± SEM: 4.2 ± 4.4 ms; $t[9] = 0.94$, $p = 0.373$). At the low pressure (250 kPa), RTs were not significantly different for anti-saccades directed by either contralateral (mean difference ± SEM: 5.5 ± 12.4 ms; $t[9] = 0.44$, $p = 0.670$) or ipsilateral (mean difference ± SEM: 2.1 ± 5.5 ms; $t[9] = 0.39$, $p = 0.707$) singleton locations. RTs were longer for pro-saccades directed by a contralateral singleton location (mean difference ± SEM: 7.9 ± 1.7 ms; $t[9] = 4.67$, $p = 0.001$) and trended toward being longer for pro-saccades directed by an ipsilateral singleton location (mean difference ± SEM: 7.1 ± 3.8 ms; $t[9] = 1.87$, $p = 0.095$).

To assess whether these effects were statistically different by location or by intensity, we performed an ANOVA with factors of location, stimulus−response rule (pro-saccade or anti-saccade) and stimulation intensity. When location was expressed as polar angle of the target location, we found that neither location ($F[7,288] = 1.06$, $p = 0.389$), stimulus−response rule ($F[1,288] = 1.54$, $p = 0.215$) or intensity ($F[1,288] = 0.361$, $p = 0.548$) affected the magnitude of the RT effect. When location was expressed as the hemifield relative to the stimulation site, we again found that neither hemifield ($F[1,232] = 3.17$, $p = 0.076$), stimulus-response

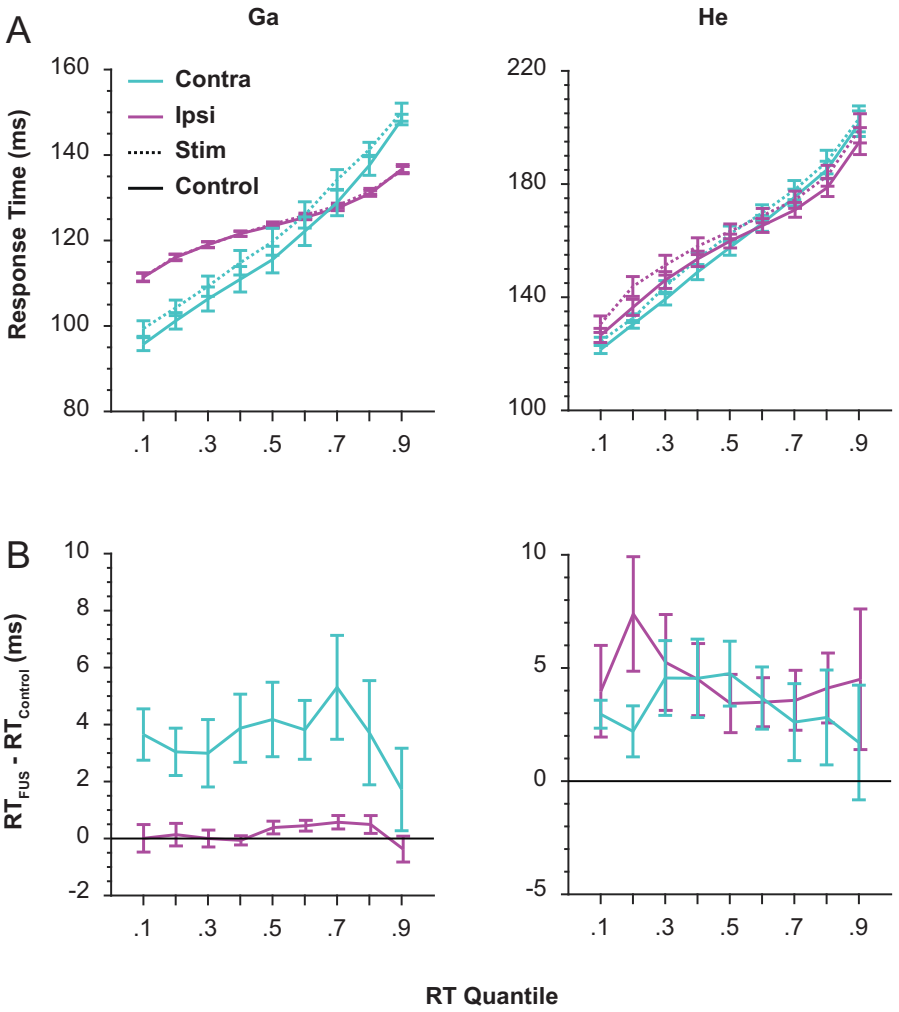

Fig. 5. Focused ultrasound (FUS) effects across response time (RT) distributions for shape singleton search task. (A) Response times for FUS trials (*dashed lines*) and no-FUS trials (*solid lines*) for contralateral singletons (*cyan*) and ipsilateral singletons (*magenta*) were divided into quantiles. The average response time quantiles across sessions are plotted. Data from monkey Ga are shown in the left column, and those for monkey He, in the right column. (B) Difference functions across quantiles. The average difference ± standard error of the mean (SEM) between FUS trials and no-FUS trials for contralateral (*cyan*) and ipsilateral (*magenta*) singletons per quantile are shown. Longer response times in FUS trials relative to no-FUS trials are above zero. Effect magnitude was invariant across RT quantiles.

rule ($F(1,232) = 0.06$, $p = 0.803$) or intensity ($F[1,232] = 1.11$, $p = 0.293$) affected the magnitude of the accuracy effect.

Because we found no overall statistical effect of intensity, we repeated the analysis combining across intensities. In the combined intensities, we found that RTs were significantly longer in pro-saccades directed by both ipsilateral singletons (mean ± SEM: 9.0 ± 3.3 ms; $t[19] = 2.72$, $p = 0.0135$) and contralateral singletons (mean ± SEM: 6.0 ± 2.3 ms; $t[19] = 2.56$, $p = 0.0191$). RTs were also significantly longer in anti-saccades directed by contralateral singletons (mean ± SEM: 18.5 ± 8.7 ms; $t[19] = 2.13$, $p = 0.0465$) but not ipsilateral singletons (mean ± SEM: 0.3 ± 3.5 ms; $t[19] = 0.10$, $p = 0.9252$).

We again divided the RT distributions from each session and each condition into quantiles and calculated the correlation between the difference between FUS and no-FUS trials and RT quantile (Fig. 7). For each condition in which an effect of FUS on mean RT was found, we also found that the effect increased across RT quantiles (ipsilateral pro-saccade singletons: $r[178] = 0.20$, $p = 0.0066$; contralateral pro-saccade singletons: $r[178] = 0.15$, $p = 0.0479$; contralateral anti-saccade singletons: $r[178] = 0.36$, $p < 0.001$). Thus, as RT increases, the effect of FUS also increases. We found no difference in RT

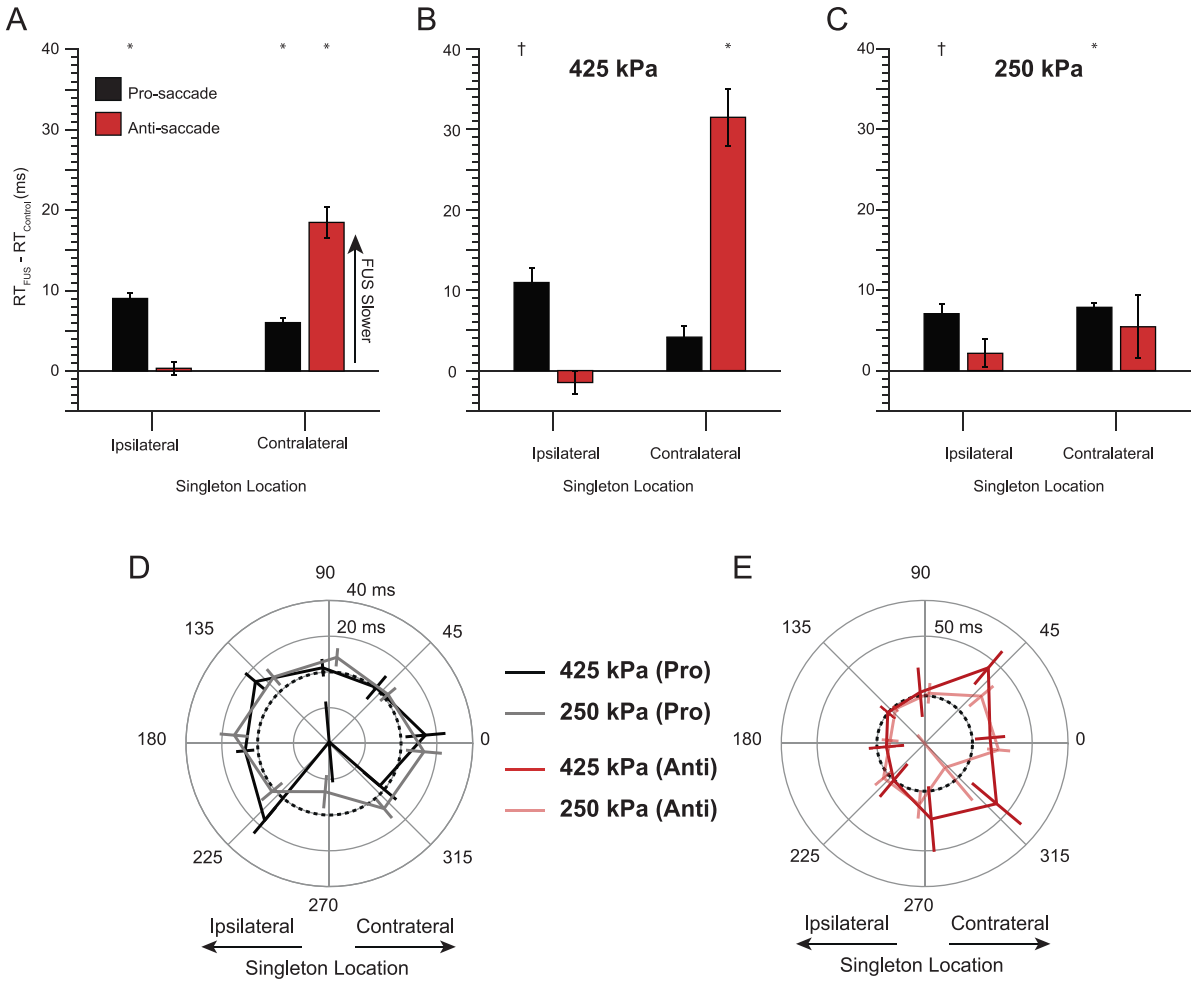

Fig. 6. Average performance for the pro-saccade/anti-saccade search task. (A) The average differences ± standard error of the mean (SEM) for response times are shown for pro-saccade trials (*black*) and anti-saccade trials (*red*). Differences are calculated separately for ipsilateral singletons (left) and contralateral singletons (right). Longer response times (RTs) in the focused ultrasound (FUS) condition relative to the no-FUS condition are plotted upward. Asterisks mark significant differences from 0 ($p < 0.05$). (B) Average differences ± SEM response times in only the high-intensity (425 kPa) trials. Conventions as in (A). †Trends toward significance ($p < 0.1$). (C) Average differences ± SEM response times in only the low-intensity (250 kPa) trials. Conventions as in (B). (D) Mean differences in pro-saccade RT for each singleton location. High-intensity sessions are in *black*, and low-intensity sessions in *gray*. A dashed black line at a 0-ms difference (no effect) is shown for reference. (E) Mean differences in anti-saccade RT for each singleton location. High-intensity sessions are in *saturated red*, and low-intensity sessions in *desaturated red*.

between FUS and no-FUS trials for ipsilateral anti-saccade singletons, nor did this difference change through RT percentile ($r[178] = 0.13$, $p = 0.0774$).

Effects of ultrasound modulation across the session

Finally, we assessed whether the effects of FUS were integrated across the session. Each session was divided into 10 quantiles, allowing analysis of the effect of ultrasound early during a session, at the end of a session and at intermediate times (Fig. 8, top and middle rows). For Ga, the effect of FUS increased throughout the session for contralateral saccades ($r[82] = 0.25$, $p = 0.0220$) but not for ipsilateral saccades ($r[82] = -0.20$, $p = 0.0623$). For He, the effect of FUS did not change throughout the session for either contralateral saccades ($r[80] = 0.04$, $p = 0.7369$) or ipsilateral saccades ($r[81] = -0.00$, $p = 0.9872$). Although the FUS effect for Ga's contralateral saccades increased throughout the session, across sessions this effect did not correlate with session length ($r[12] = 0.26$, $p = 0.8415$). For Ga's ipsilateral saccades and all of He's saccades, session length and FUS effect magnitude did not correlate (Ga right: $[r[12] = -0.06$, $p = 0.8361$; He left: $r[12] = 0.06$, $p = 0.8415$; He right: $r[12] = -0.31$, $p = 0.2818$). To rule out that the repeated FUS stimulation could have caused damage to FEF, we tested for

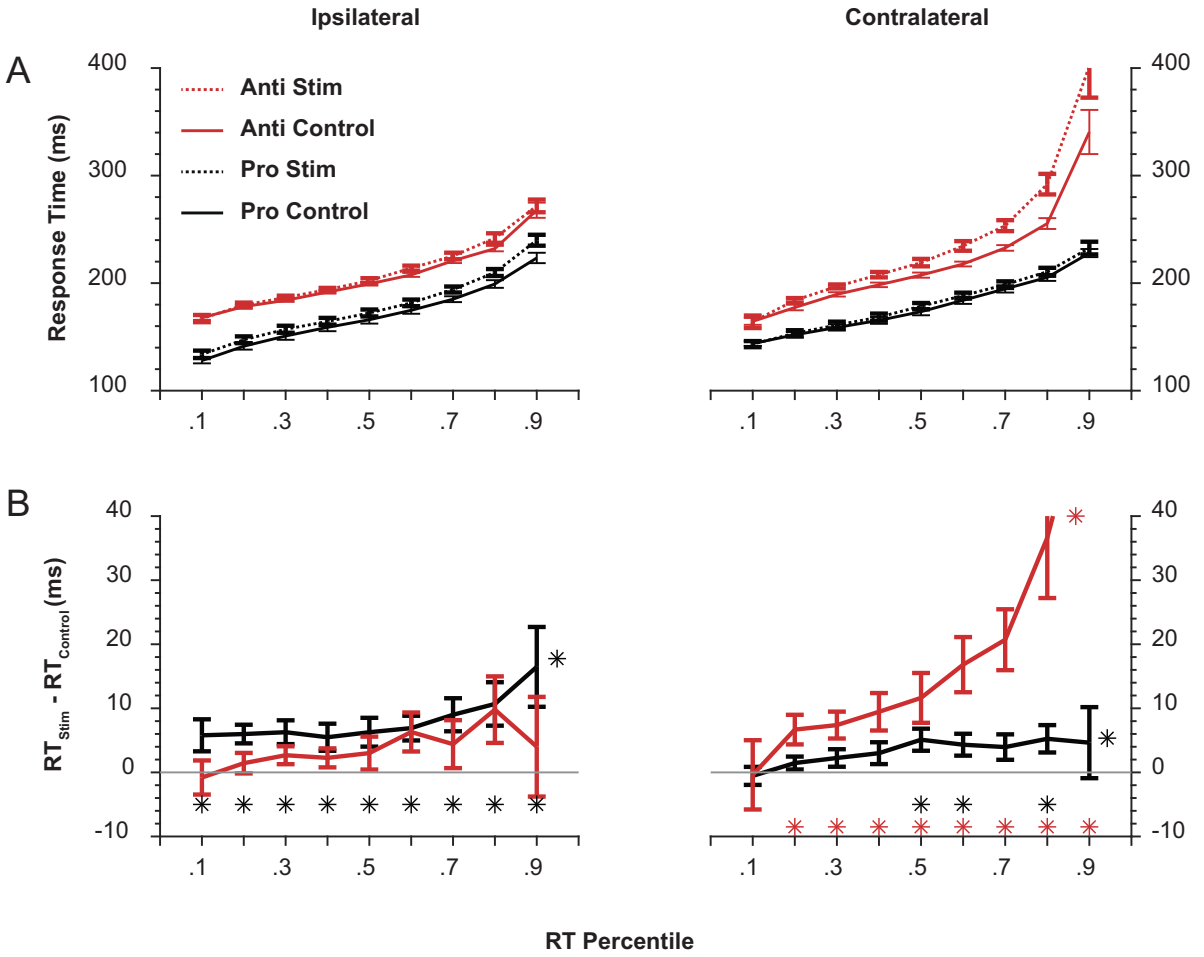

Fig. 7. Focused ultrasound (FUS) effects across response time (RT) distributions for the pro-saccade/anti-saccade search task. (A) Average ± standard error of the mean (SEM) RTs for FUS trials (*dashed lines*) and no-FUS trials (*solid lines*) for pro-saccade (*black*) and anti-saccade (*red*) trials were divided into quantiles. The average ± SEM RT quantiles are plotted for ipsilateral singleton locations (left) and contralateral anti-saccade locations (right). (B) Average ± SEM difference functions across quantiles are plotted for pro-saccade (*black*) and anti-saccade (*red*) trials. Ipsilateral singleton locations are shown on the left, and contralateral singleton locations on the right. Asterisks below lines indicate significant differences from zero for pro-saccade quantiles (*black asterisks,* $p < 0.05$) and anti-saccade quantiles (*red asterisks,* $p < 0.05$). Asterisks to the right of a curve indicate a significant correlation between FUS effect and RT quantile. Contralateral anti-saccade differences at the 0.9 quantile exceed the range of the ordinate.

performance impairments across sessions by checking for linear trends in the RT data and error rates. Both animals performing the visual search task, Ga and He, did not exhibit a clear relationship between session number on RT (Ga: $r[12] = 0.01$, $p = 0.9707$; He: $r[12] = 0.40$, $p = 0.1538$) nor accuracy (Ga: $r[12] = 0.12$, $p = 0.6898$; He: $r[12] = 0.22$, $p = 0.4465$).

For the third monkey (monkey Da), the effect of the ultrasound did not change across the session (Fig. 8, bottom row). The difference between FUS and no-FUS trials did not correlate with session quantiles for ipsilateral pro-saccade singleton saccades ($r[194] = 0.004$, $p = 0.9547$), contralateral pro-saccade singleton saccades ($r[196] = -0.056$, $p = 0.4311$), ipsilateral anti-saccade singletons ($r[192] = -0.019$, $p = 0.7891$) or contralateral anti-saccade singletons ($r[191)] = 0.106$, $p = 0.1421$). Further, the three conditions affected by FUS were not affected by session length. Session length did not correlate with the difference between FUS and no-FUS trials for ipsilateral pro-saccade singletons ($r[18] = -0.28$, $p = 0.2347$), contralateral pro-saccade singletons ($r[18] = -0.19$, $p = 0.4115$) or contralateral anti-saccade singletons ($r[18] = -0.24$, $p = 0.3086$). We also tested whether ultrasound affected overall RTs or accuracy across sessions. We did not find any relationship between session number and overall RT ($r[18] = 0.22$,

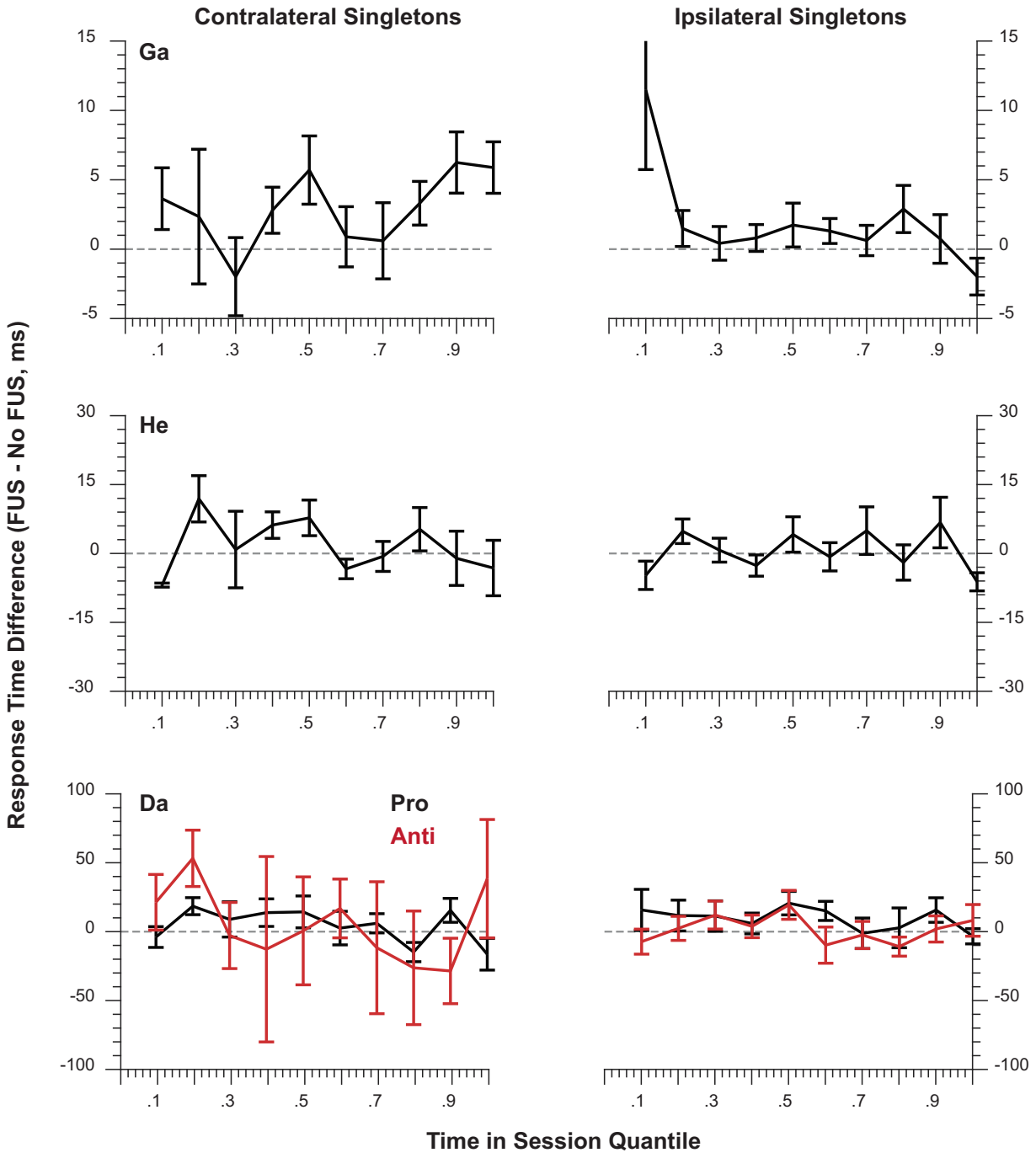

Fig. 8. Focused ultrasound (FUS) effects across session quantiles for all three monkeys. Each session was divided into 10 time quantiles (*i.e.,* for a 3-h session, time in session quantile 0.1 is the first 18 min, whereas for a 2-h session, time in session quantile 0.1 is the first 12 min, *etc.*). Average ± standard error of the mean (SEM) response time (RT) differences between FUS and no-FUS trials at each time quantile are shown. Contralateral singletons are shown in the left column, and ipsilateral singletons, in the right column. Monkeys Ga (top row) and He (middle row) performed the shape singleton search task. For this task, all RT differences are shown in *black*. Monkey Da (bottom row) performed the pro-saccade/anti-saccade search task. RT differences on pro-saccade trials are shown in *black,* and those on anti-saccade trials are shown in *red. Dashed gray lines* at a 0-ms RT difference (*i.e.,* no difference) are shown for reference.

$p = 0.3515$), nor did we find any relationship between session number and overall accuracy ($r[18] = -0.09$, $p = 0.7028$).

DISCUSSION

Acoustic neuromodulation *via* FUS has gained popularity with respect to spatially specific invasive but direct stimulation techniques and spatially general but non-invasive techniques (Yoo et al. 2011). The role of the FEF in performance of visual search has long been established and recent studies have reported the effects of FUS modulation of this circuit in macaques (Deffieux et al. 2013; Wattiez et al. 2017). These premises motivated the use of FUS over FEF in assessing the impact of this new technique on visuomotor behavior. Our study adds to prior knowledge in this field by directly coupling to the dura, removing uncertainties with acoustic transmission through the skull and potential confounds with known somatosensory effects of ultrasound in the skin (Legon et al. 2012). We found that this direct coupling to the dura is effective in modulating visuomotor transformations in the FEF as assayed by modulation of behavior in complex cognitive tasks.

One consistent finding in the present data is that FUS prolongs response times for saccades cued by contralateral stimuli. As FEF neurons have spatially constrained receptive fields that are concentrated in the contralateral hemisphere (Bruce and Goldberg 1985; Schall 1991), it is likely that FUS interfered with processing of contralateral visual stimuli. However, it should also be noted that monkeys He (Fig. 3) and Da (Fig. 6) also exhibited delayed responses for saccades toward ipsilateral targets. This rules out a mechanism of FUS that simply drives or inhibits saccades in the contralateral direction. Importantly, for anti-saccades, the location of the singleton was important; only when located in the contralateral hemifield was a clear slowing of RT observed at high FUS intensity, but if the informative stimulus was in the ipsilateral hemifield, no slowing of RT was observed for both FUS intensities. Our finding is similar to previous studies of FUS applied to the FEF (Deffieux et al. 2013; Wattiez et al. 2017). These results further suggest that FUS affects the visual components of FEF processing and not motor components.

However, these previous studies found no effects of FUS stimulation on pro-saccade response times (Deffieux et al. 2013; Wattiez et al. 2017). Here, all three monkeys exhibited a response slowing toward targets located in the contralateral hemifield. This could be due to differences in stimulation protocols. Our stimulations were 300 ms in duration, whereas the previous stimulations were 100 ms, and our stimulations occurred before or alongside the array onset. Alternatively, differences could be due to the increased complexity of the search tasks used in the present study, which require comparisons of stimuli across the visual field as opposed to detection of a single stimulus. This suggests that exclusive interpretation of visual effects of FUS are premature. Rather, effects are likely due to a disruption of the visuomotor transformation.

Another notable difference between the previous studies and the present data is the intensity of stimulation. The previous study used a pressure of 600 kPa, whereas we used a pressure of 425 or 250 kPa. However, their stimulation was not coupled directly to the dura and instead stimulated transcranially. This difference in procedure may have allowed for a larger effective pressure reaching into FEF tissue, whereas in the previous study the bone would have absorbed some of the stimulation strength. This may also explain why we did not observe differences between the two stimulation intensities; the direct coupling to the dura may have allowed for neuromodulation sufficient to induce behavioral changes even by the lower pressure stimulation. Alternately, in our tasks, multiple stimuli were compared at once, which places a higher demand on FEF (as opposed to the one stimulus presented by Deffieux et al. (2013) or the two-choice stimuli presented by Kubanek et al. (2020); during search, FEF neurons are active during an initial visual transient even when the target is not in the neurons' response field, whereas those neurons are not active when a detection target is outside the response field (Schall et al. 1995). As such, this higher demand may lower the modulation threshold for behavioral relevance as the underlying computations are more complex.

The mechanisms by which FUS produces neuromodulation are unclear and debated (Tyler 2011; Naor et al. 2016; Plaksin et al. 2016; Oh et al. 2019). However, because of the mechanical nature of acoustic waves, FUS may differentially affect larger pyramidal cells or smaller interneurons (Naor et al. 2016). If the different neuron populations are crucial for specific functions it is possible that FUS could affect brain functions differently. For example, there are anatomic differences between functionally defined categories of FEF neurons (Cohen et al. 2009). Thus, if FUS differentially affects anatomic subtypes then it may differentially affect neurons that are exclusively visually responsive, neurons that are exclusively related to saccade production or neurons that are responsive to both aspects of visuomotor behavior (Bruce and Goldberg 1985; Schall 1991; Lowe and Schall 2018). As the functional neuron classes are also differentially distributed across the cortical layers (Segraves and Goldberg 1987), FUS stimulation could have different effects if it is focused on different layers. In our study, we removed the bone that could lead to a deterioration of the beam focus, and therefore

we are able to produce a much cleaner focus of the ultrasound beam. Future studies are needed to leverage the spatial specificity to characterize behavioral differences of the FUS modulation depending on the targeted layers.

Some limitations of our study should be considered when interpreting our results. Effects caused by stimulation of neighboring brain regions are a concern for all non-invasive neuromodulation modes, and auditory confounds are the primary concern during FUS neuromodulation. Although we avoided potential somatosensory stimulation in the skull or skin by sonicating through the craniotomy, we did not control for potential auditory confounds that have been observed in rodent models (Guo et al. 2018; Sato et al. 2018). Stimulation of cochlear fluids is thought to underlie auditory effects in rodent models, but the beam emitted from transducers in our study would not extend to the non-human primate cochlea because of the larger head size compared to rodents.

Alternately, the skull is known to conduct sound at ultrasonic frequencies (Abramovich 1978), so sonicating through the craniotomy likely reduced some auditory confounds. Further, these auditory or tactile effects would manifest predominantly in the ipsilateral direction *via* an orienting response. However, because the FUS we observed was dependent on the singleton location in two of the monkeys, we can be more confident that these potential auditory or tactile confounds, which should be location invariant, are not responsible for the present results. Nevertheless, an improved study would attempt to prevent auditory confounds or auditory distractor stimulus by using smooth amplitude windows (Mohammadjavadi et al. 2019) or ramping waveforms (*e.g.,* Deffieux et al. 2013).

While these considerations aid in the interpretation of the present results, additional studies would consider using transcranial methods to exploit the advantage of FUS being non-invasive and to validate and generalize the results. FUS has been applied to FEF transcranially and produced behaviorally relevant effects (Deffieux et al. 2013; Kubanek et al. 2020). In this study, FUS was instead applied through existing craniotomies. There has been work to correct for beam aberrations and provide steering capabilities: multi-element array transducers can counteract the effects of the skull on the ultrasound beam to recover much of the natural focus (Kyriakou et al. 2014). Similarly, acoustic lens methods have been developed to account for beam aberration while still using inexpensive single-element transducers (Maimbourg et al. 2018, 2020).

In sum, these data indicate that FEF stimulation *via* FUS is effective in modulating behavior in cognitively demanding tasks. The use of these demanding tasks provides evidence that FUS affects either the visual processing or the visuomotor transformation, not strictly the motor circuitry. Though the effects are not clear-cut, some particular findings are consistent. These findings are promising and validate use of the FEF as a substrate for exploring the mechanisms and limits of FUS for neuromodulation.

Acknowledgments—This work was supported by NIH grants R24 MH109105, R01MH111877, NEI P30-EY008126 and U54-HD083211 and by Robin and Richard Patton through the E. Bronson Ingram Chair in Neuroscience. The authors also thank Jillian Shuman for her technical assistance during data collection.

Conflict of interest disclosure—The authors declare no conflicts of interest.

REFERENCES

Abramovich SJ. Auditory perception of ultrasound in patients with sensorineural and conductive hearing loss. J Laryngol Otol 1978;92: 861–867.

Berényi A, Belluscio M, Mao D, Buzsák G. Closed-loop control of epilepsy by transcranial electrical stimulation. Science 2012;337: 735–737.

Blackmore J, Shrivastava S, Sallet J, Butler CR, Cleveland RO. Ultrasound neuromodulation: A review of results, mechanisms and safety. Ultrasound Med Biol 2019;45:1509–1536.

Bruce CJ, Goldberg ME. Primate frontal eye fields: I. Single neurons discharging before saccades. J Neurophysiol 1985;53:603–635.

Cohen JY, Pouget P, Heitz RP, Woodman GF, Schall JD. Biophysical support for functionally distinct cell types in the frontal eye field. J Neurophysiol 2009;101:912–916.

Cosman JD, Lowe KA, Zinke W, Woodman GF, Schall JD. Prefrontal control of visual distraction. Curr Biol 2018;28 414−420.e3.

Deffieux T, Younan Y, Wattiez N, Tanter M, Pouget P, Aubry JF. Low-intensity focused ultrasound modulates monkey visuomotor behavior. Curr Biol 2013;23:2430–2433.

Guo H, Hamilton M, Offutt SJ, Gloeckner CD, Li T, Kim Y, Legon W, Alford JK, Lim HH. Ultrasound produces extensive brain activation via a cochlear pathway. Neuron 2018;98 1020−1030.e4.

Huerta MF, Krubitzer LA, Kaas JH. Frontal eye field as defined by intracortical microstimulation in squirrel monkeys, owl monkeys, and macaque monkeys: I. Subcortical connections. J Comp Neurol 1986;253:415–439.

Huerta MF, Krubitzer LA, Kaas JH. Frontal eye field as defined by intracortical microstimulation in squirrel monkeys, owl monkeys, and macaque monkeys: II. Cortical connections. J Comp Neurol 1987;265:332–361.

Kubanek J, Brown J, Ye P, Pauly KB, Moore T, Newsome W. Remote, brain region-specific control of choice behavior with ultrasonic waves. Sci Adv 2020;6(21) eaaz4193.

Kyriakou A, Neufeld E, Werner B, Paulides MM, Szekely G, Kuster N. A review of numerical and experimental compensation techniques for skull-induced phase aberrations in transcranial focused ultrasound. Int J Hyperthermia 2014;30:36–46.

Legon W, Rowlands A, Opitz A, Sato TF, Tyler WJ. Pulsed ultrasound differentially stimulates somatosensory circuits in humans as indicated by EEG and fMRI. PLoS One 2012;7:e51177.

Lowe KA, Schall JD. Functional categories of visuomotor neurons in macaque frontal eye field. ENeuro 2018;5(5) ENEURO.0131-18.2018.

Maimbourg G, Houdouin A, Deffieux T, Tanter M, Aubry JF. 3D-printed adaptive acoustic lens as a disruptive technology for transcranial ultrasound therapy using single-element transducers. Phys Med Biol 2018;63 025026.

Maimbourg G, Houdouin A, Deffieux T, Tanter M, Aubry JF. Steering capabilities of an acoustic lens for transcranial therapy: Numerical and experimental studies. IEEE Trans Biomed Eng 2020;67:27–37.

Mayberg HS, Lozano AM, Voon V, McNeely HE, Seminowicz D, Hamani C, Schwalb JM, Kennedy SH. Deep brain stimulation for treatment-resistant depression. Neuron 2005;45:651–660.

Mohammadjavadi M, Ye PP, Xia A, Brown J, Popelka G, Pauly KB. Elimination of peripheral auditory pathway activation does not affect motor responses from ultrasound neuromodulation. Brain Stimul 2019;12:901–910.

Nahas Z, Lomarev M, Roberts DR, Shastri A, Lorberbaum JP, Teneback C, McConnell K, Vincent DJ, Li X, George MS, Bohning DE. Unilateral left prefrontal transcranial magnetic stimulation (TMS) produces intensity-dependent bilateral effects as measured by interleaved BOLD fMRI. Biol Psychiatry 2001;50:712–720.

Naor O, Krupa SL, Shoham S. Ultrasonic neuromodulation. J Neural Eng 2016;13 031003.

Oh SJ, Lee JM, Kim HB, Lee J, Han S, Bae JY, Hong GS, Koh W, Kwon J, Hwang ES, Woo DH, Youn I, Cho IJ, Bae YC, Lee S, Shim JW, Park JH, Lee CJ. Ultrasonic neuromodulation via astrocytic TRPA1. Curr Biol 2019;29 3386-3401.e8.

Plaksin M, Kimmel E, Shoham S. Cell-type-selective effects of intramembrane cavitation as a unifying theoretical framework for ultrasonic neuromodulation. ENeuro 2016;3(3) ENEURO.0136-15.2016.

Pollak TA, Nicholson TR, Edwards MJ, David AS. A systematic review of transcranial magnetic stimulation in the treatment of functional (conversion) neurological symptoms. J Neurol Neurosurg Psychiatry 2014;85:191–197.

Sato TR, Schall JD. Effects of stimulus−response compatibility on neural selection in frontal eye field. Neuron 2003;38:637–648.

Sato T, Shapiro MG, Tsao DY. Ultrasonic neuromodulation causes widespread cortical activation via an indirect auditory mechanism. Neuron 2018;98 1031−1041.e5.

Schall JD. Neuronal activity related to visually guided saccades in the frontal eye fields of rhesus monkeys: Comparison with supplementary eye fields. J Neurophysiol 1991;66:559–579.

Schall JD. Visuomotor functions in the frontal lobe. Annu Rev Vision Sci 2015;1:469–498.

Schall JD, Hanes DP, Thompson KG, King DJ. Saccade target selection in frontal eye field of macaque: I. Visual and premovement activation. J Neurosci 1995;15:6905–6918.

Segraves MA, Goldberg ME. Functional properties of corticotectal neurons in the monkey's frontal eye field. J Neurophysiol 1987;58:1387–1419.

Stanton GB, Goldberg ME, Bruce CJ. Frontal eye field efferents in the macaque monkey: II. Topography of terminal fields in midbrain and pons. J Comp Neurol 1988;271:493–506.

Tyler WJ. Noninvasive neuromodulation with ultrasound? A continuum mechanics hypothesis. Neuroscientist 2011;17:25–36.

Wattiez N, Constans C, Deffieux T, Daye PM, Tanter M, Aubry JF, Pouget P. Transcranial ultrasonic stimulation modulates single-neuron discharge in macaques performing an antisaccade task. Brain Stimul 2017;10:1024–1031.

Yoo SS, Bystritsky A, Lee JH, Zhang Y, Fischer K, Min BK, McDannold NJ, Pascual-Leone A, Jolesz F. A. Focused ultrasound modulates region-specific brain activity. NeuroImage 2011;56:1267–1275.